

Reducing Unimodal Bias in Multi-Modal Semantic Segmentation with Multi-Scale Functional Entropy Regularization

Xu Zheng^{1,2} Yuanhuiyi Lyu¹ Lutao Jiang¹
Danda Pani Paudel² Luc Van Gool² Xuming Hu^{1,3,*}

¹AI Thrust, HKUST(GZ) ²INSAIT, Sofia University “St. Kliment Ohridski” ³CSE, HKUST

Abstract

Fusing and balancing multi-modal inputs from novel sensors for dense prediction tasks, particularly semantic segmentation, is critically important yet remains a significant challenge. One major limitation is the tendency of multi-modal frameworks to over-rely on easily learnable modalities, a phenomenon referred to as **unimodal dominance or bias**. This issue becomes especially problematic in real-world scenarios where the dominant modality may be unavailable, resulting in severe performance degradation. To this end, we apply a **simple but effective** plug-and-play regularization term based on functional entropy, which introduces no additional parameters or modules. This term is designed to intuitively balance the contribution of each visual modality to the segmentation results. Specifically, we leverage the log-Sobolev inequality to bound functional entropy using functional-Fisher-information. By maximizing the information contributed by each visual modality, our approach mitigates unimodal dominance and establishes a more balanced and robust segmentation framework. A multi-scale regularization module is proposed to apply our proposed plug-and-play term on high-level features and also segmentation predictions for more balanced multi-modal learning. Extensive experiments on three datasets demonstrate that our proposed method achieves superior performance, i.e., **+13.94%**, **+3.25%** and **+3.64%**, without introducing any additional parameters.

1. Introduction

Multi-modal dense prediction tasks, especially for semantic segmentation [3–13], rely on integrating complementary inputs from diverse sensors (e.g., RGB, depth, thermal, event cameras) to achieve robust scene understanding [2, 14, 15]. While such fusion promises resilience to real-world variability, a critical challenge persists: models often exhibit

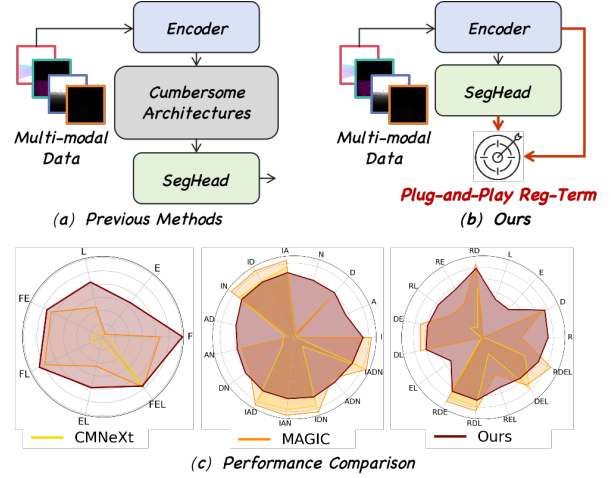


Figure 1. (a) Previous methods use complex architectures to fuse multi-modal data. (b) Our approach **simplifies** the architecture and use plug-and-play regularization terms. The results show significant improvements of ours than CMNeXt [1] and MAGIC [2].

unimodal bias, disproportionately favoring one modality over others [16, 17]. For instance, in RGB-thermal segmentation, RGB inputs—common in training pipelines—often dominate predictions, even in low-light conditions where thermal data is crucial. Similarly, systems combining event cameras with conventional sensors may under-utilize the motion-aware edge information from event cameras in dynamic scenes, defaulting to static RGB inputs. This imbalance occurs when models prioritize the most easily learned or information-rich modality, neglecting others. As a result, performance degrades when the dominant modality is missing (e.g., RGB corruption) or unreliable (e.g., thermal sensor noise), posing risks in safety-critical applications like autonomous navigation.

Prior multi-modal methods often fail to explicitly regulate how modalities contribute to predictions [1], leaving models vulnerable to over-reliance on dominant in-

*Corresponding author.

puts. Functional entropy addresses this gap by quantifying the uncertainty in a model’s dependence on modalities: *a system with high entropy distributes its “attention” evenly across sensors, while low entropy indicates undue reliance on a single modality*. Inspired by functional entropy which has been successfully applied in visual question answering task [18], we apply this concept to the challenging multi-modal semantic segmentation. However, directly applying the regularization is *non-trivial* because the multi-modal semantic segmentation task presents significant challenges in enabling the model to learn pixel-wise multi-modal representations while balancing the contributions of multiple modalities, in contrast to the dual-modality and VQA task addressed in [18].

In this paper, we apply the simple yet effective plug-and-play regularization terms at multiple scales of the segmentation model to balance various visual modalities while encourage equal multi-modal learning. As shown in Fig. 1 (c), framing modality balance as an entropy maximization problem, these regularization terms reduce bias and ensure equitable sensor utilization, crucial for segmentation accuracy when modalities degrade or fail. Unlike complex architectures [2, 15], we draw from recent multi-modal learning advancements [19], which show that intricate connectors are increasingly unnecessary. This suggests that sophisticated fusion mechanisms are not required. We propose a simpler approach: instead of adding fusion modules, we treat all input modalities equally within a mini-batch, achieving fusion by averaging predictions, avoiding unnecessary complexity in the segmentation backbone.

To implement the proposed regularization term in multi-modal semantic segmentation tasks, we introduce a multi-scale regularization module that takes both multi-scale features and predictions into consideration. The prediction-level regularization is to ensure that predictions across different modalities are consistent, thereby encouraging the model to integrate information across modalities in a balanced manner. Meanwhile, the regularization with the multi-scale feature aims to enforce smoothness and balance, making sure that no single scale or modality disproportionately influences the final output.

Extensive experiments on real-world and synthetic benchmarks demonstrate the superior robustness and performance of our method compared to existing state-of-the-art approaches, achieving mIoU improvements of +13.94%, +3.25% and +3.64% respectively. Additionally, we conduct series of ablation studies to show how the proposed regularization terms work. Our contributions are as follows: **(I)** We introduce functional entropy-based regularization to mitigate unimodal bias and ensure balanced multi-modal learning, reducing reliance on any single modality. **(II)** We propose a straightforward multi-modal fusion framework that averages input modalities within a mini-batch, avoid-

ing complex fusion modules and simplifying the segmentation backbone. **(III)** Our regularization terms are applied at both feature and prediction levels, effectively balancing multi-modal training. Extensive experiments show robust performance across various benchmarks.

2. Related Work

2.1. Multi-modal Semantic Segmentation

Multi-modal Semantic Segmentation seeks to combine RGB with complementary modalities such as depth [20–33], thermal [34–44], events [45–49], and LiDAR [50–57]. Advances in sensor technology have driven significant progress in multi-modal fusion [20, 48, 58–64], evolving from dual-modality to comprehensive multi-modal systems, like MCubeSNet [65], which improves scene understanding by utilizing richer sensor data.

From an architectural standpoint, multi-modal fusion models are generally classified into three categories: separate branches [35, 66–68], joint branches [27, 52], and asymmetric branches [1, 69]. A common approach in these models is to treat RGB as the primary modality, while auxiliary sensors provide additional information. For instance, CMNeXT [1] prioritizes RGB, incorporating other sensors to supplement the data. However, RGB alone may be insufficient, particularly in challenging conditions like low light or nighttime. This limitation highlights the need for more robust fusion models that leverage the strengths of multiple modalities, minimizing dependence on any single sensor. In this context, Liu *et al.* [70] introduced the concept of modality-incomplete scene segmentation, addressing deficiencies at both the system and sensor levels.

2.2. Unimodal Bias

As shown in Fig. 2, a key challenge in multi-modal tasks, especially for multi-modal semantic segmentation, is unimodal bias, where models favor one modality over others, leading to suboptimal performance. For instance, as shown in Tab. 2, the frame camera has a dominant effect on the performance of most methods. Specifically, when the frame camera is included in the evaluation, the performance significantly increases. However, when it is missing, the performance drops sharply. This bias arises when models prioritize the most easily learnable or information-rich modality under specific conditions, neglecting the complementary benefits of other modalities. This can lead to a significant degradation in performance when the dominant modality is missing or unreliable [2, 15, 70], such as in cases of RGB corruption or thermal sensor noise, which can be particularly problematic for safety-critical applications like autonomous navigation. Several strategies have been proposed to address unimodal bias in multi-modal learning [2, 15]. Traditional multi-modal fusion models often do

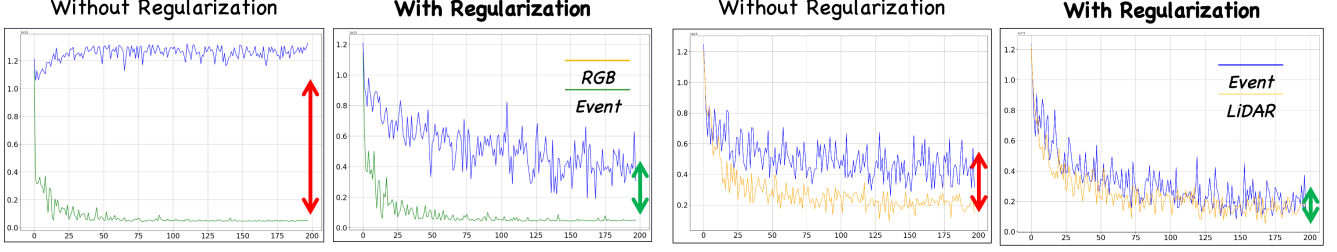


Figure 2. Visualization of Fisher information during training with real-world MUSES (right) and synthetic DELIVER (left) datasets. Adding a regularization term *reduces the gap* between modality Fisher information values. With regularization, the model utilizes both input modalities, resulting in *closer modality distances*. Without regularization, the model relies more on RGB in the first two rows and Event in the last two, increasing the modality distance (red arrows).

not explicitly regulate how each modality contributes to the final predictions, which can lead to over-reliance on a single input. Recent works, such as MAGIC [2] and Any2Seg [15] have sought to address this limitation by introducing well-designed training objectives.

In multi-modal learning, methods [16, 17] often draw from information theory, particularly the concept of functional entropy [18]. Entropy-based approaches quantify a model’s uncertainty in its reliance on different modalities. A system with high entropy distributes its “attention” evenly across modalities, while low entropy signals an over-reliance on a single modality. Building on the application of functional Fisher information in visual question answering tasks [18], directly applying this approach to semantic segmentation presents challenges. Unlike visual question answering, which focuses on interpreting questions based on a single modality, segmentation tasks require the integration of both spatial and contextual information across multiple modalities. To address this, we introduce multi-scale regularization terms at both the feature and prediction levels. These regularization terms provide a principled framework to mitigate unimodal bias, encouraging a more balanced utilization of all available sensors. This ensures that models maintain accuracy even in scenarios where certain modalities degrade or fail—an essential consideration in environments with unreliable or variable sensor performance.

3. Method

This paper focuses on multi-modal visual data from novel sensors, where each instance in a data batch x consists of multiple modalities. For instance, in multi-modal semantic segmentation [1], RGB images provide color and texture information, depth maps capture geometric details, event cameras offer motion cues, and LiDAR provides accurate point clouds. A mini-batch of data from these modalities can be represented as: $x = \{x_r, x_d, x_e, x_l\}$, where each modality resides in its own Euclidean space, i.e., $x_i \in \mathbb{R}^d$. Here, x_r represents the RGB, x_d represents the depth, x_e represents the event, and x_l represents the LiDAR modality,

with each x_i being a vector in a d -dimensional space. The goal of multi-modal semantic segmentation is to optimize the parameters w of a function that assigns a probability score to each possible label y given the input mini-batch x .

3.1. Reducing Unimodal Dominance / Bias

In the context of multi-modal semantic segmentation, existing methods [1, 2, 15] introduce additional modules and parameters to encourage balanced training across multiple visual modalities. However, neural networks often tend to overly rely on a single modality, leading to significant challenges in real-world scenarios. For instance, as shown in Tab. 2, the frame camera has a dominant effect on the performance of most methods. Specifically, when the frame camera is included in the evaluation, the performance significantly improves. However, its absence results in a sharp decline in performance. This phenomenon, commonly referred to as *unimodal dominance* or *bias*, occurs when the learned function disproportionately emphasizes the most easily learnable modality, potentially neglecting critical information from other modalities.

3.1.1. Functional Entropy

In multi-modal learning, functional entropy quantifies the uncertainty and variability in the model’s multi-modal predictions and representation [18]. Let $f(x)$ represent the model’s prediction for a multi-modal input mini-batch $x = \{x_r, x_d, x_e, x_l\}$, where $x \in \mathbb{R}^d$ includes RGB, Depth, LiDAR, and Event data. The functional entropy of a non-negative function $f(x) \geq 0$ is defined as:

$$\text{Ent}_\mu(f) = \int_{\mathbb{R}^d} f(x) \log f(x) d\mu(x) - \left(\int_{\mathbb{R}^d} f(x) d\mu(x) \right) \log \left(\int_{\mathbb{R}^d} f(x) d\mu(x) \right), \quad (1)$$

where $f(x)$ represents the model’s predictions in the form of segmentation logits and multi-scale features, which reflect how the model combines different modalities. Here,

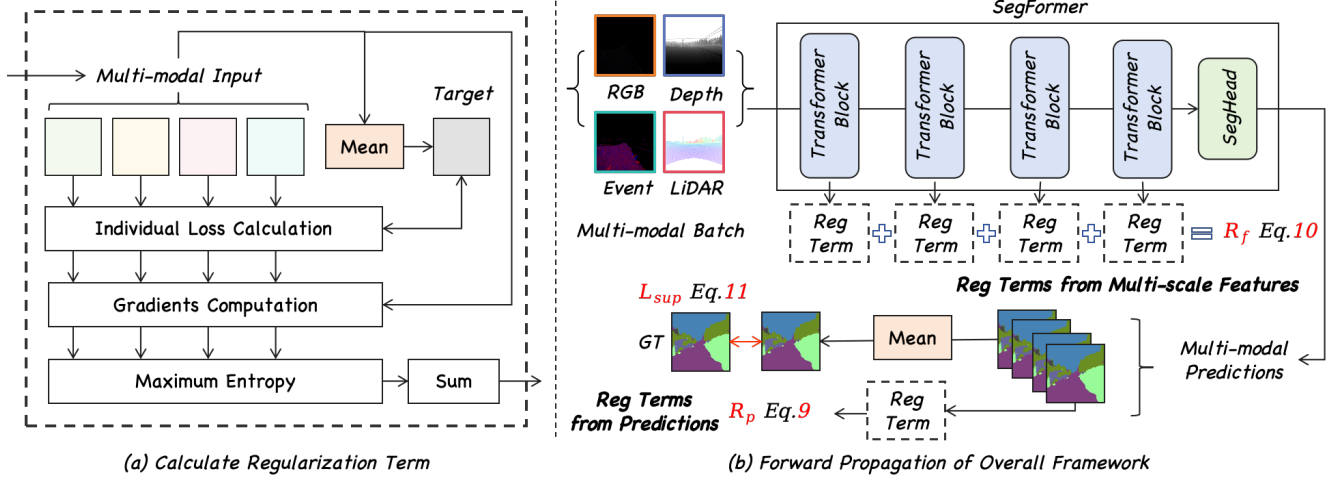


Figure 3. (a) The proposed regularization term for multi-modal input and (2) overall framework of our proposed multi-scale regularization terms' implementation.

μ represents a probability measure defined over the Euclidean space \mathbb{R}^d . This measure describes the distribution of the multi-modal inputs, quantifying how likely each point (pixel in prediction logits or element from high-level features) in the input space is, typically based on a distribution over \mathbb{R}^d . As shown in Fig. 2, a low entropy suggests over-reliance on a single modality (e.g., RGB), while higher entropy indicates better modality integration (e.g., RGB, Depth, LiDAR, Event data).

During training, we apply random modality dropout to expose the model to diverse input combinations. Let $x' = \{x_1, x_2, \dots, x_i\}$ represent the available modalities during training, where $1, 2, \dots, i \in \{r, d, e, l\}$ are a subset of modalities (RGB, Depth, Event, LiDAR), and $n \leq 4$. This accounts for missing modalities by excluding corresponding terms from the input. For a non-negative function $f(x')$, the functional entropy is bounded as:

$$\text{Ent}_\mu(f) \leq \frac{1}{2} \int_{\mathbb{R}^d} \frac{\|\nabla f(x')\|^2}{f(x')} d\mu(x'), \quad (2)$$

where $\|\nabla f(x')\|$ is the gradient of $f(x')$. Large Fisher information values indicate a model's dependence on specific modalities (e.g., RGB), suggesting a need for better modality integration, even with missing inputs.

Different from [18], which focuses solely on the image-level visual question answering task using only image and text modalities, we aim to address the **more complex pixel-level understanding task by incorporating multiple visual modalities**. Simply increasing the utilization of the visual modality in visual question answering is straightforward; however, when multiple visual modalities are integrated with pixel-level tasks such as semantic segmentation, the problem becomes far more challenging. These challenges stem not only from improving the utilization of the

visual modality but also from effectively balancing multiple modalities. To better handle multi-modal data, we decompose the overall functional entropy across modalities, allowing the model to independently assess the contribution of each modality. This is crucial when some modalities are missing during training or inference. By isolating the impact of each modality, the model can adapt to modality-missing scenarios more effectively. For a multi-modal segmentation model, the functional entropy is bounded as:

$$\text{Ent}_\mu(f^x) \leq \sum_{i=1}^n \text{Ent}_{\mu_i}(f(x_i)), \quad (3)$$

where μ_i is the marginal distribution for modality x_i . This decomposition enables the model to focus on each modality's role, improving efficiency and flexibility. As a result, the model provides more accurate predictions even when some modalities are missing or incomplete.

3.1.2. Regularization

To enhance multi-modal integration and prevent modality dominance, the regularization term is:

$$\mathcal{R} = \lambda \sum_{i=1}^n \left(\int_{\mathbb{R}^{d_i}} \frac{\|\nabla_{x_i} \text{CE}(p_w(\cdot|x_i), p_w(\cdot|x))\|^2}{\text{CE}(p_w(\cdot|x_i), p_w(\cdot|x))} d\mu_i(x_i) \right)^{-1} \quad (4)$$

where λ controls regularization strength. This regularization term serves to promote smoother predictions and ensures a more balanced contribution from all modalities. By discouraging over-reliance on any single modality—such as the frame camera, which may underperform in low-light conditions—it encourages the use of complementary modalities. For instance, depth data aids in capturing geometric information, while LiDAR offers enhanced precision. However, directly estimating functional entropy from

the equation presents practical challenges. To address this, we leverage the log-Sobolev inequality for Gaussian measures, which provides a bound on functional entropy via functional Fisher information. This approach implicitly encourages the maximization of information across modalities. To implement this, we utilize the inverse of the information derived from Equation 4, thereby promoting a more equitable contribution from each modality. The efficacy of this regularization method is demonstrated in Fig. 2, where it improves the stability and robustness of the multi-modal segmentation process.

3.2. Overall Framework

3.2.1. Overview

The concepts of functional entropy and functional Fisher information provide a theoretical foundation for analyzing and improving multi-modal semantic segmentation. By quantifying how different modalities are integrated and balanced, these measures address modality dominance, leading to more robust and generalized predictions. This approach is particularly important in multi-modal tasks, where leveraging the complementary strengths of each modality is essential for accurate segmentation.

Recent advancements in multi-modal learning models, such as Qwen2-VL [19], have shown that the need for complex connectors in multi-modal architectures is diminishing. Early models, such as ViLT, demonstrated that simple linear projections could effectively process image data for Transformers. More recent lightweight models have adopted multi-layer perceptrons (MLPs) to handle visual inputs, sometimes eliminating dedicated visual encoders altogether. These trends suggest that sophisticated fusion mechanisms are not necessarily required for effective multi-modal integration. Building on these insights, we propose a straightforward approach: instead of using additional fusion modules, we treat all input visual modalities equally within a single mini-batch. Multi-modal fusion is achieved simply by taking the mean of the input modalities, *without complicating the backbone semantic segmentation framework*.

In the forward pass, the multi-modal mini-batch $x = \{x_r, x_d, x_e, x_l\}$ is processed directly by the encoder within the backbone, producing multi-scale, high-level feature representations $\{f_r^j, f_d^j, f_l^j, f_e^j\}_{j=1}^4$ as well as the prediction segmentation maps $\{p_r, p_d\}$ for the respective modalities. This operation is formulated as:

$$\{f_r^j, f_d^j\}_{j=1}^4, \{p_r, p_d\} = F(\{r, d\}), \quad (5)$$

where j corresponds to the feature level derived from the j -th transformer block of the encoder. The final prediction p for the input multi-modal mini-batch x is obtained by averaging the individual modality predictions: $p = \text{Mean}(p_r, p_d)$.

Table 1. Results with dual (RGB-Depth) modalities on DELIVER dataset. † denotes the MMS method from [70] and ‡ follows [71].

Method	RGB-Depth Fusion			Mean
	RGB-Depth	RGB-Dpeth	RGB-Depth	
CMNeXt [1]	1.60	1.44	63.58	22.81
CMNeXt ‡	32.97	48.53	61.93	47.81
CMNeXt †	<u>53.39</u>	53.73	62.24	<u>56.45</u>
MultiMAE [72]	24.60	38.55	58.94	40.70
MultiMAE ‡	19.24	42.54	56.62	39.47
MultiMAE †	52.46	45.62	58.68	52.25
FPT [70]	50.73	39.60	57.38	49.24
MAGIC [2]	37.26	<u>59.02</u>	66.89	54.39
Ours	55.04	59.60	<u>66.46</u>	60.37

3.2.2. Multi-scale Regularization Module

To implement the proposed regularization term in multi-modal semantic segmentation tasks, we introduce a multi-scale regularization module that takes both multi-scale features and predictions into consideration. This module encourages balanced learning at both the feature and prediction levels, ensuring that all modalities contribute equally to the final segmentation output across all scales.

Regularization with Predictions: We introduce a regularization term at the prediction level. The objective is to ensure that predictions at different scales are consistent, thereby encouraging the model to integrate information across modalities in a balanced manner. The regularization term for predictions can be written as:

$$\mathcal{R}_p = \lambda_p \sum_{i=1}^n \left(\int_{\mathbb{R}^{d_i}} \frac{\|\nabla_{x_i} \text{CE}(p, gt)\|^2}{\text{CE}(p, gt)} d\mu_i(x_i) \right)^{-1}, \quad (6)$$

where gt represents the ground truth for the semantic segmentation, and p is the predicted output. λ_p is a regularization parameter controlling the strength of the prediction-level regularization. This term penalizes inconsistencies in predictions across different modalities, encouraging the model to produce balanced outputs.

Regularization with Features: As Fig. 3 shows, we take the multi-scale features $\{f_r^j, f_d^j\}_{j=1}^4$ from the segmentation backbone model to perform feature-level functional entropy-based regularization. This regularization enforces smoothness and balance across the multi-scale features, ensuring that no single scale or modality disproportionately influences the final output. The regularization term for features can be formulated as:

$$\mathcal{R}_f = \lambda_f \sum_{j=1}^4 \sum_{i=1}^n \left(\int_{\mathbb{R}^{d_i}} \frac{\|\nabla_{f_i} \text{CE}(\{f_r^j, f_d^j\}, f_m^j)\|^2}{\text{CE}(\{f_r^j, f_d^j\}, f_m^j)} d\mu_i(f_i^j) \right)^{-1}, \quad (7)$$

where λ_f is a regularization parameter that controls the strength of the feature-level regularization, and f_j repre-

Table 2. Results of segmentation validation with three modalities (frame: F, event: E, and LiDAR: L) on MUSES [73].

Method	Training with All Modalities and Evaluation with Different Combinations							Mean
	F	E	L	FE	FL	EL	FEL	
CMX [74]	2.52	2.35	3.01	41.15	41.25	2.56	42.27	19.30
CMNeXt [1]	3.50	2.77	2.64	6.63	10.28	3.14	46.66	10.80
MAGIC [2]	43.22	2.68	22.95	43.51	49.05	22.98	49.02	33.34
Any2Seg [15]	44.40	3.17	22.33	44.51	49.96	22.63	50.00	33.86
Ours	60.33	33.15	42.59	47.19	53.47	39.59	47.89	47.80

Table 3. Results of segmentation validation with four modalities (RGB: R, Depth: D, Event: E, and LiDAR: L) on DELIVER [1].

Method	Training with All Modalities and Evaluation with Different Combinations															Mean
	R	D	E	L	RD	RE	RL	DE	DL	EL	RDE	RDL	REL	DEL	RDEL	
CMNeXt [1]	0.86	0.49	0.66	0.37	47.06	9.97	13.75	2.63	1.73	2.85	59.03	59.18	14.73	59.18	39.07	20.77
MAGIC [2]	32.60	55.06	0.52	0.39	63.32	33.02	33.12	55.16	55.17	0.26	63.37	63.36	33.32	55.26	63.40	40.49
Any2Seg [15]	39.02	60.11	2.07	0.31	68.21	39.11	39.04	60.92	60.15	1.99	68.24	68.22	39.06	60.95	68.25	45.04
Ours	55.56	57.74	32.40	34.26	59.69	47.70	47.78	48.99	50.26	34.37	53.42	54.12	45.24	47.33	51.65	48.29

sents the features extracted at the j -th scale. The regularization encourages consistency and smoothness in feature representations across different scales, preventing any one scale from dominating the learning process.

3.3. Training Objectives

The supervised loss uses the cross-entropy between the predicted labels p and the ground truth gt , as follows:

$$\mathcal{L}_{sup} = \text{CE}(p, gt). \quad (8)$$

To ensure that the model generalizes effectively and integrates multi-modal information in a balanced manner, the overall training objective is formulated as a combination of the supervised loss and the regularization terms:

$$\mathcal{L} = \mathcal{L}_{sup} + \mathcal{R}_p + \mathcal{R}_f, \quad (9)$$

where \mathcal{R}_p and \mathcal{R}_f are the regularization terms that ensure consistency and smoothness in the model’s predictions and features, respectively.

4. Experiments

Datasets. We evaluate our method using synthetic and real-world multi-sensor datasets. The MUSES dataset [75] provides data from a high-resolution frame camera, event camera, and MEMS LiDAR, supporting robust multimodal semantic segmentation with high-quality 2D panoptic labels for benchmarking. The DELIVER dataset [1] includes RGB, depth, LiDAR, and event data across 25 categories, capturing diverse environmental conditions and sensor failures. MCubeS [65] is a material segmentation dataset with 20 categories and pairs of RGB, Near-Infrared (NIR),

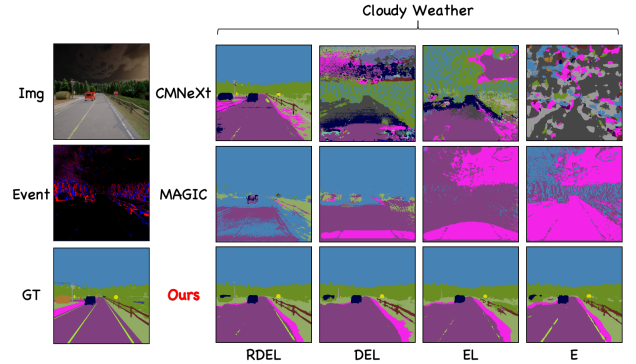


Figure 4. Visualization on DELIVER [1] with [1] and [2].

DoLP, and AoLP images. **Implementation Details.** All experiments were conducted on 8 NVIDIA GPUs. The initial learning rate was set to 6×10^{-5} and adjusted using a polynomial decay strategy with a power of 0.9 over 200 epochs. More details can be found in the *suppl. mat.*.

4.1. Results

Tab. 1 presents results on DELIVER [1] using dual (RGB-Depth) modalities. Our method outperforms others with a mean score of 60.37%. Compared to MAGIC, we improve by +7.98% in RGB-Depth fusion and +6.99% in the overall mean, demonstrating strong performance across both modalities. Tab. 2 shows results on MUSES [75]. Our method achieves mIoU values of 60.33% for frame, 33.15% for event, and 42.59% for LiDAR, with a mean mIoU of 47.80%, surpassing prior methods. Compared to the pre-

Table 4. Results of segmentation validation with four modalities (I: Image, Aolp: A, Dolp: D, and Nir: N) on MCubeS [65].

Method	Training with All Modalities and Evaluation with Different Combinations															Mean
	I	A	D	N	IA	ID	IN	AD	AN	DN	IAD	IAN	IDN	ADN	IADN	
CMNeXt [1]	1.86	1.54	2.51	2.28	47.96	43.67	45.90	6.99	7.58	9.95	50.07	48.77	48.83	8.06	51.54	25.17
MAGIC [2]	51.91	0.32	34.52	2.66	52.24	52.16	52.57	1.98	36.01	37.09	52.48	52.82	52.73	37.57	53.01	38.00
Ours	46.21	37.66	40.49	40.56	43.93	43.11	43.73	40.10	39.19	40.72	41.78	41.53	42.21	40.63	42.73	41.64

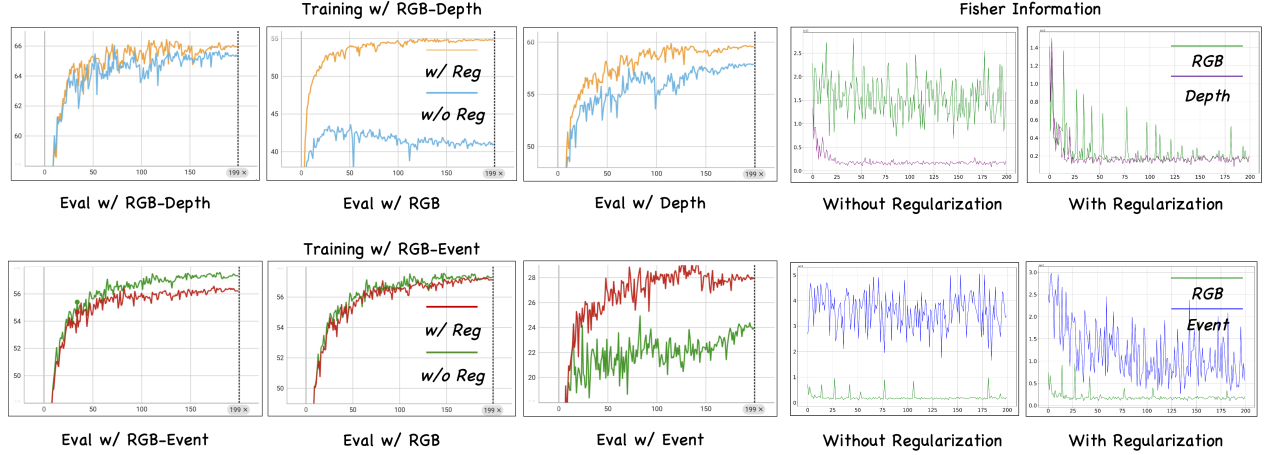


Figure 5. Comparison of model performance with (w/) and without (w/o) our proposed prediction level regularization term across different modalities (RGB-Depth, RGB, and RGB-Event).

vious SoTA, we achieve a mean mIoU improvement of +13.94%, showcasing superior performance in both uni-modal and multimodal tasks. Tab. 3 reports results on DELIVER [1]. We achieve 55.56% for RGB, 57.74% for Depth, 32.40% for Event, and 34.26% for LiDAR. Paired modality combinations also perform well, with results of 59.69% for RGB-Depth (RD), 47.70% for RGB-Event (RE), 47.78% for RL, 48.99% for DE, 50.26% for DL, and 34.37% for EL. These results demonstrate the robustness of our method across cross-modal relationships. As in Tab. 4, our method outperforms CMNeXt and MAGIC with a mIoU of 41.64%, compared to MAGIC’s 38.00% and CMNeXt’s 25.17%. We observe significant improvements in segmentation validation for combinations such as Image and Aolp, with an average increase of +3.64% over SoTA methods. Fig. 4 shows qualitative results on DELIVER, where our method outperforms across various loss combinations and conditions. These results validate our method’s ability to effectively leverage diverse modalities.

5. Ablation

Effectiveness of Loss Functions Tab. 5 presents the results of different loss function combinations on the MUSES dataset. Introducing \mathcal{L}_{Rp} improves performance, particularly for paired modalities. The mean mIoU increases to 50.02%, with a +29.44% gain for the event modality. Al-

though the frame modality slightly decreases to 59.63%, the overall result improves due to substantial gains in the event (+29.44%) and both modalities (+61.00%). Including \mathcal{L}_{Rf} , yields a consistent performance improvement across all modalities. The mean mIoU rises to 50.44%, with gains of +29.66% for the frame, +61.02% for event, and +50.44% for both modalities.

Effectiveness of Regularization Term. As shown in Fig. 5, the results demonstrate consistent improvement with regularization. For example, in the RGB-Depth combination, the model with regularization (w/ Reg) reaches 65% at 150 epochs, outperforming the model without regularization (w/o Reg), which peaks at 62%. A similar trend is observed in RGB-Event. Fisher Information plots further confirm these results, showing that without regularization, the model over-relies on individual modalities, as indicated by higher Fisher information values for RGB and Event. With regularization, Fisher information is more balanced across modalities, indicating better utilization of both inputs. This balance is particularly evident in RGB-Depth and RGB-Event combinations, where modality distances decrease with regularization. Overall, these findings highlight the effectiveness of regularization in promoting balanced modality usage, improving stability, and enhancing performance in multi-modal tasks.

Ablation of Multi-scale Feature-level Regularization The

Table 5. Ablation of different loss combinations on MUSES.

Optimization			mIoU			Mean	Acc			Mean
L_{sup}	R_p	R_f	Frame	Event	Both		Frame	Event	Both	
✓	-	-	60.63	6.48	60.70	42.60	71.34	14.92	71.32	52.53
✓	✓	-	59.63	29.44	61.00	50.02	68.89	39.39	74.01	60.76
✓	✓	✓	60.63	29.66	61.02	50.44	69.98	39.98	74.49	61.48

Table 6. Sensitivity analysis on the effect of different values of λ_p on MUSES [75].

λ_p	mIoU			Mean	Acc			Mean
	F	E	FE		F	E	FE	
0.0	57.93	28.68	58.84	48.48	67.95	37.98	72.58	59.50
0.1	58.45	29.64	59.43	49.17	68.23	38.78	73.05	60.02
0.3	59.06	29.95	60.67	49.89	68.48	39.96	73.93	60.79
0.5	57.82	29.31	59.81	48.98	67.04	38.28	73.26	59.53
0.7	57.60	29.04	59.01	48.55	67.19	38.89	72.76	59.61

Table 7. Ablation on the effect of different λ_f on MUSES [75].

λ_p	mIoU			Mean	Acc			Mean
	F	E	FE		F	E	FE	
0.0	59.06	29.95	60.67	49.89	68.48	39.96	73.93	60.79
0.02	60.63	29.66	61.02	50.44	69.88	39.98	74.49	61.45
0.04	59.96	30.09	60.74	50.26	69.38	40.44	74.29	61.37
0.06	58.84	31.08	60.16	50.03	68.62	40.96	74.05	61.21

results in Fig. 6 compare the performance of two regularization strategies: the Pred-level Reg-Term (left) and the combined Feat- & Pred-level Reg-Term (right). The comparison clearly shows that incorporating multi-scale regularization results in a smoother reduction of Fisher information over time, as seen in the right plot. In contrast, the left plot with only prediction-level regularization exhibits more fluctuations, indicating less stable convergence. This ablation emphasizes the significance of multi-scale feature-level regularization, as it improves stability and effectiveness, leading to smoother training dynamics and enhanced generalization across modalities.

Hyper-parameters Tables 6 and 7 show the impact of λ_p and λ_f on the MUSES dataset. In Table 6, $\lambda_p = 0.3$ achieves the best performance with a mIoU of 59.06% and accuracy of 60.79%, outperforming other values. Lower values (0.0 and 0.1) result in slightly worse performance, while higher values (0.5 and 0.7) show a decrease, especially in frame modality. Table 7 demonstrates that $\lambda_f = 0.02$ gives the best results, with a mIoU of 60.63% and accuracy of 61.45%. Larger λ_f values (0.04 and 0.06) cause a slight performance drop. These findings highlight the importance of tuning λ_p and λ_f , with $\lambda_p = 0.3$ and $\lambda_f = 0.02$

Table 8. Ablation of training efficiency with 8 H100 GPUs.

	w/o Reg Terms	w/ Reg Terms
Training Time (hours)	2.462	2.476 (0.014↑)

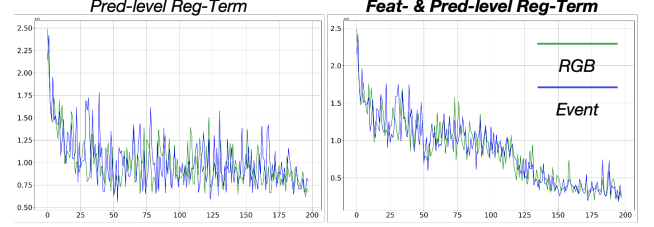


Figure 6. Ablation of the effectiveness of multi-scale feature-level regularization.

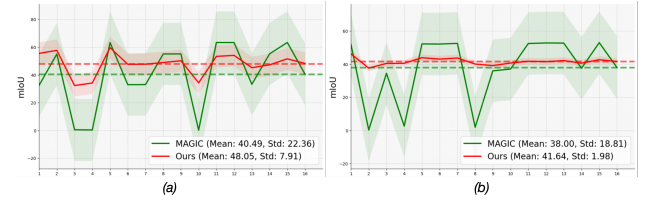


Figure 7. Balanced multi-modal performance comparison between ours and MAGIC [2] on (a) DELIVER and (b) MCubeS.

yielding the best results.

6. Discussion

Differences with [18]. Unlike [18], which focuses on image-level visual question answering with image and text modalities, we address the more complex pixel-level task by incorporating multiple visual modalities. Challenges arise from both improving modality utilization and balancing multiple modalities. When we directly apply the regularization term from [18], the resulting mIoU on MUSES is 42.89%, significantly lower than our 50.44%.

Unimodal Bias. As in Fig. 7, compared to MAGIC [2] (green line), which exhibits a notable unimodal bias, our method (red line) demonstrates consistent performance across modality combinations. MAGIC shows a mean mIoU of 40.49% with a high standard deviation of 22.36, reflecting sensitivity to certain modality pairs. In contrast, our method achieves a higher mean mIoU of 48.05% with a smaller standard deviation of 7.91, highlighting its robustness and stability. This trend emphasizes the absence of unimodal bias in our approach, as it handles all modality combinations effectively, unlike MAGIC, which suffers from significant fluctuations. The shaded areas around the curves further emphasize the reduced variability of our method, demonstrating its stability and reliability in achieving balanced performance across modalities.

Training Efficiency As shown in Tab. 8, we compare the training efficiency of the model with and without regularization terms across 8 NVIDIA GPUs. The results show a slight increase in training time, with the model using regularization taking 2.476 hours, compared to 2.462 hours without regularization—an increase of 0.014 hours (approximately 0.57%). Despite this minimal increase, the performance improvements justify the inclusion of regularization, offering a favorable trade-off between efficiency and accuracy. Thus, regularization proves to be a valuable investment with negligible impact on training time.

7. Conclusion

We presented a simple yet effective regularization term based on functional entropy to mitigate unimodal bias in multi-modal semantic segmentation. Our approach ensures balanced utilization of all input modalities, improving robustness in scenarios where some modalities are unavailable or degraded. Extensive experiments on synthetic and real-world benchmarks demonstrated significant performance improvements, achieving better results without introducing extra parameters or complexity. Key contributions include introducing a novel regularization technique, proposing a simple fusion framework, and applying entropy maximization for balanced multi-modal learning. Our method outperforms existing approaches, offering a practical solution for robust multi-modal integration with multiple visual modalities. Future work could extend this approach to other multi-modal tasks for robust and stable scene understanding.

References

- [1] J. Zhang, R. Liu, H. Shi, K. Yang, S. Reiß, K. Peng, H. Fu, K. Wang, and R. Stiefelhausen, “Delivering arbitrary-modal semantic segmentation,” in *Proceedings of the IEEE/CVF Conference on Computer Vision and Pattern Recognition*, pp. 1136–1147, 2023. [1](#), [2](#), [3](#), [5](#), [6](#), [7](#)
- [2] X. Zheng, Y. Lyu, J. Zhou, and L. Wang, “Centering the value of every modality: Towards efficient and resilient modality-agnostic semantic segmentation,” in *ECCV*, pp. 192–212, Springer, 2025. [1](#), [2](#), [3](#), [5](#), [6](#), [7](#), [8](#)
- [3] E. Xie, W. Wang, Z. Yu, A. Anandkumar, J. M. Alvarez, and P. Luo, “Segformer: Simple and efficient design for semantic segmentation with transformers,” *Advances in neural information processing systems*, vol. 34, pp. 12077–12090, 2021. [1](#)
- [4] J. Chen, D. Deguchi, C. Zhang, X. Zheng, and H. Murase, “Frozen is better than learning: A new design of prototype-based classifier for semantic segmentation,” *Pattern Recognition*, vol. 152, p. 110431, 2024.
- [5] X. Zheng, Y. Luo, P. Zhou, and L. Wang, “Distilling efficient vision transformers from cnns for semantic segmentation,” *arXiv:2310.07265*, 2023.
- [6] X. Zheng, C. Fu, H. Xie, J. Chen, X. Wang, and C. Sham, “Uncertainty-aware deep co-training for semi-supervised medical image segmentation,” *Comput. Biol. Medicine*, vol. 149, p. 106051, 2022.
- [7] J. Chen, C. Fu, H. Xie, X. Zheng, R. Geng, and C. Sham, “Uncertainty teacher with dense focal loss for semi-supervised medical image segmentation,” *Comput. Biol. Medicine*, vol. 149, p. 106034, 2022.
- [8] J. Zhou, X. Zheng, Y. Lyu, and L. Wang, “Exact: Language-guided conceptual reasoning and uncertainty estimation for event-based action recognition and more,” *CoRR*, vol. abs/2403.12534, 2024.
- [9] H. Xie, C. Fu, X. Zheng, Y. Zheng, C. Sham, and X. Wang, “Adversarial co-training for semantic segmentation over medical images,” *Comput. Biol. Medicine*, vol. 157, p. 106736, 2023.
- [10] X. Zheng, P. Zhou, A. V. Vasilakos, and L. Wang, “Semantics, distortion, and style matter: Towards source-free UDA for panoramic segmentation,” in *IEEE/CVF Conference on Computer Vision and Pattern Recognition, CVPR 2024, Seattle, WA, USA, June 16-22, 2024*, pp. 27885–27895, IEEE, 2024.
- [11] B. Ren, Y. Li, J. Liang, R. Ranjan, M. Liu, R. Cucchiara, L. V. Gool, M.-H. Yang, and N. Sebe, “Sharing key semantics in transformer makes efficient image restoration,” *Advances in Neural Information Processing Systems*, vol. 37, pp. 7427–7463, 2024.
- [12] B. Ren, Y. Liu, Y. Song, W. Bi, R. Cucchiara, N. Sebe, and W. Wang, “Masked jigsaw puzzle: A versatile position embedding for vision transformers,” in *Proceedings of the IEEE/CVF Conference on Computer Vision and Pattern Recognition*, pp. 20382–20391, 2023.
- [13] B. Ren, G. Mei, D. P. Paudel, W. Wang, Y. Li, M. Liu, R. Cucchiara, L. Van Gool, and N. Sebe, “Bringing masked autoencoders explicit contrastive properties for point cloud self-supervised learning,” in *Proceedings of the Asian Conference on Computer Vision*, pp. 2034–2052, 2024. [1](#)
- [14] X. Zheng, Y. Liu, Y. Lu, T. Hua, T. Pan, W. Zhang, D. Tao, and L. Wang, “Deep learning for event-based vision: A comprehensive survey and benchmarks,” *arXiv:2302.08890*, 2023. [1](#)
- [15] X. Zheng, Y. Lyu, and L. Wang, “Learning modality-agnostic representation for semantic segmentation from any modalities,” in *European Conference on Computer Vision*, pp. 146–165, Springer, 2024. [1](#), [2](#), [3](#), [6](#)
- [16] Y. Zhang, P. E. Latham, and A. M. Saxe, “Understanding unimodal bias in multimodal deep linear networks,” in *International Conference on Machine Learning*, 2024. [1](#), [3](#)
- [17] X. Zheng, H. Xue, J. Chen, Y. Yan, L. Jiang, Y. Lyu, K. Yang, L. Zhang, and X. Hu, “Learning robust anymodal segmentor with unimodal and cross-modal distillation,” *arXiv preprint arXiv:2411.17141*, 2024. [1](#), [3](#)
- [18] I. Gat, I. Schwartz, A. Schwing, and T. Hazan, “Removing bias in multi-modal classifiers: Regularization by maximizing functional entropies,” *Advances in Neural Information Processing Systems*, vol. 33, pp. 3197–3208, 2020. [2](#), [3](#), [4](#), [8](#)
- [19] P. Wang, S. Bai, S. Tan, S. Wang, Z. Fan, J. Bai, K. Chen, X. Liu, J. Wang, W. Ge, *et al.*, “Qwen2-vl: Enhancing vision-language model’s perception of the world at any resolution,” *arXiv preprint arXiv:2409.12191*, 2024. [2](#), [5](#)

- [20] Y. Lyu, X. Zheng, D. Kim, and L. Wang, "Omnibind: Teach to build unequal-scale modality interaction for omni-bind of all," *arXiv:2405.16108*, 2024. 2
- [21] Y. Lyu, X. Zheng, J. Zhou, and L. Wang, "Unibind: Llm-augmented unified and balanced representation space to bind them all," in *Proceedings of IEEE/CVF CVPR*, pp. 26752–26762, 2024.
- [22] Y. Lyu, X. Zheng, and L. Wang, "Image anything: Towards reasoning-coherent and training-free multi-modal image generation," *arXiv:2401.17664*, 2024.
- [23] Y. Wang, F. Sun, M. Lu, and A. Yao, "Learning deep multimodal feature representation with asymmetric multi-layer fusion," in *Proceedings of the 28th ACM MM*, pp. 3902–3910, 2020.
- [24] H. Zhou, L. Qi, Z. Wan, H. Huang, and X. Yang, "Rgb-d co-attention network for semantic segmentation," in *Proceedings of the ACCV*, 2020.
- [25] Y. Wang, W. Huang, F. Sun, T. Xu, Y. Rong, and J. Huang, "Deep multimodal fusion by channel exchanging," *NeurIPS*, vol. 33, pp. 4835–4845, 2020.
- [26] J. Cao, H. Leng, D. Lischinski, D. Cohen-Or, C. Tu, and Y. Li, "Shapeconv: Shape-aware convolutional layer for indoor rgb-d semantic segmentation," in *Proceedings of the IEEE/CVF ICCV*, pp. 7088–7097, 2021.
- [27] L.-Z. Chen, Z. Lin, Z. Wang, Y.-L. Yang, and M.-M. Cheng, "Spatial information guided convolution for real-time rgbd semantic segmentation," *IEEE TIP*, vol. 30, pp. 2313–2324, 2021. 2
- [28] X. Ying and M. C. Chuah, "Ucnet: Uncertainty-aware cross-modal transformer network for indoor rgb-d semantic segmentation," in *ECCV*, pp. 20–37, Springer, 2022.
- [29] M. Lee, C. Park, S. Cho, and S. Lee, "Spsn: Superpixel prototype sampling network for rgb-d salient object detection," in *ECCV*, pp. 630–647, Springer, 2022.
- [30] R. Cong, Q. Lin, C. Zhang, C. Li, X. Cao, Q. Huang, and Y. Zhao, "Cir-net: Cross-modality interaction and refinement for rgb-d salient object detection," *IEEE TIP*, vol. 31, pp. 6800–6815, 2022.
- [31] W. Ji, G. Yan, J. Li, Y. Piao, S. Yao, M. Zhang, L. Cheng, and H. Lu, "Dmra: Depth-induced multi-scale recurrent attention network for rgb-d saliency detection," *IEEE TIP*, vol. 31, pp. 2321–2336, 2022.
- [32] F. Wang, J. Pan, S. Xu, and J. Tang, "Learning discriminative cross-modality features for rgb-d saliency detection," *IEEE TIP*, vol. 31, pp. 1285–1297, 2022.
- [33] M. Song, W. Song, G. Yang, and C. Chen, "Improving rgb-d salient object detection via modality-aware decoder," *IEEE TIP*, vol. 31, pp. 6124–6138, 2022. 2
- [34] S. S. Shivakumar, N. Rodrigues, A. Zhou, I. D. Miller, V. Kumar, and C. J. Taylor, "Pst900: Rgb-thermal calibration, dataset and segmentation network," in *2020 IEEE ICRA*, pp. 9441–9447, IEEE, 2020. 2
- [35] Q. Zhang, S. Zhao, Y. Luo, D. Zhang, N. Huang, and J. Han, "Abmdrnet: Adaptive-weighted bi-directional modality difference reduction network for rgb-t semantic segmentation," in *Proceedings of the IEEE/CVF Conference on Computer Vision and Pattern Recognition*, pp. 2633–2642, 2021. 2
- [36] W. Wu, T. Chu, and Q. Liu, "Complementarity-aware cross-modal feature fusion network for rgb-t semantic segmentation," *Pattern Recognition*, vol. 131, p. 108881, 2022.
- [37] G. Liao, W. Gao, G. Li, J. Wang, and S. Kwong, "Cross-collaborative fusion-encoder network for robust rgb-thermal salient object detection," *IEEE TCSVT*, vol. 32, no. 11, pp. 7646–7661, 2022.
- [38] W. Zhou, H. Zhang, W. Yan, and W. Lin, "Mmsmcnet: Modal memory sharing and morphological complementary networks for rgb-t urban scene semantic segmentation," *IEEE TCSVT*, 2023.
- [39] Z. Xie, F. Shao, G. Chen, H. Chen, Q. Jiang, X. Meng, and Y.-S. Ho, "Cross-modality double bidirectional interaction and fusion network for rgb-t salient object detection," *IEEE TCSVT*, 2023.
- [40] G. Chen, F. Shao, X. Chai, H. Chen, Q. Jiang, X. Meng, and Y.-S. Ho, "Modality-induced transfer-fusion network for rgb-d and rgb-t salient object detection," *IEEE TCSVT*, vol. 33, no. 4, pp. 1787–1801, 2022.
- [41] Y. Pang, X. Zhao, L. Zhang, and H. Lu, "Caver: Cross-modal view-mixed transformer for bi-modal salient object detection," *IEEE TIP*, vol. 32, pp. 892–904, 2023.
- [42] T. Hui, Z. Xun, F. Peng, J. Huang, X. Wei, X. Wei, J. Dai, J. Han, and S. Liu, "Bridging search region interaction with template for rgb-t tracking," in *Proceedings of IEEE/CVF CVPR*, pp. 13630–13639, 2023.
- [43] T. Zhang, H. Guo, Q. Jiao, Q. Zhang, and J. Han, "Efficient rgb-t tracking via cross-modality distillation," in *Proceedings of IEEE/CVF CVPR*, pp. 5404–5413, 2023.
- [44] J. Zhao, F. Teng, K. Luo, G. Zhao, Z. Li, X. Zheng, and K. Yang, "Unveiling the potential of segment anything model 2 for rgb-thermal semantic segmentation with language guidance," *CoRR*, vol. abs/2503.02581, 2025. 2
- [45] I. Alonso and A. C. Murillo, "Ev-segnet: Semantic segmentation for event-based cameras," in *Proceedings of IEEE/CVF CVPR Workshops*, pp. 0–0, 2019. 2
- [46] J. Zhang, K. Yang, and R. Stiefelhagen, "Issafe: Improving semantic segmentation in accidents by fusing event-based data," in *2021 IEEE/RSJ International Conference on Intelligent Robots and Systems (IROS)*, pp. 1132–1139, IEEE, 2021.
- [47] X. Zheng and L. Wang, "Eventdance: Unsupervised source-free cross-modal adaptation for event-based object recognition," in *Proceedings of the IEEE/CVF Conference on Computer Vision and Pattern Recognition*, pp. 17448–17458, 2024.
- [48] J. Cao, X. Zheng, Y. Lyu, J. Wang, R. Xu, and L. Wang, "Chasing day and night: Towards robust and efficient all-day object detection guided by an event camera," *arXiv:2309.09297*, 2023. 2
- [49] J. Zhou, X. Zheng, Y. Lyu, and L. Wang, "Exact: Language-guided conceptual reasoning and uncertainty estimation for event-based action recognition and more," in *Proceedings of the IEEE/CVF Conference on Computer Vision and Pattern Recognition*, pp. 18633–18643, 2024. 2
- [50] Z. Zhuang, R. Li, K. Jia, Q. Wang, Y. Li, and M. Tan, "Perception-aware multi-sensor fusion for 3d lidar seman-

- tic segmentation,” in *Proceedings of the IEEE/CVF ICCV*, pp. 16280–16290, 2021. [2](#)
- [51] X. Yan, J. Gao, C. Zheng, C. Zheng, R. Zhang, S. Cui, and Z. Li, “2dpass: 2d priors assisted semantic segmentation on lidar point clouds,” in *ECCV*, pp. 677–695, Springer, 2022.
- [52] Y. Wang, X. Chen, L. Cao, W. Huang, F. Sun, and Y. Wang, “Multimodal token fusion for vision transformers,” in *Proceedings of the IEEE/CVF Conference on Computer Vision and Pattern Recognition*, pp. 12186–12195, 2022. [2](#)
- [53] Y. Li, A. W. Yu, T. Meng, B. Caine, J. Ngiam, D. Peng, J. Shen, Y. Lu, D. Zhou, Q. V. Le, *et al.*, “Deepfusion: Lidar-camera deep fusion for multi-modal 3d object detection,” in *Proceedings of IEEE/CVF CVPR*, pp. 17182–17191, 2022.
- [54] S. Borse, M. Klingner, V. R. Kumar, H. Cai, A. Almuzairee, S. Yogamani, and F. Porikli, “X-align: Cross-modal cross-view alignment for bird’s-eye-view segmentation,” in *Proceedings of the IEEE/CVF WACV*, pp. 3287–3297, 2023.
- [55] B. Zhang, Z. Wang, Y. Ling, Y. Guan, S. Zhang, and W. Li, “Mx2m: Masked cross-modality modeling in domain adaptation for 3d semantic segmentation,” in *Proceedings of the AAAI*, vol. 37, pp. 3401–3409, 2023.
- [56] H. Liu, T. Lu, Y. Xu, J. Liu, W. Li, and L. Chen, “Camliflow: Bidirectional camera-lidar fusion for joint optical flow and scene flow estimation,” in *Proceedings of IEEE/CVF CVPR*, pp. 5791–5801, 2022.
- [57] J. Li, H. Dai, H. Han, and Y. Ding, “Mseg3d: Multi-modal 3d semantic segmentation for autonomous driving,” in *Proceedings of the IEEE/CVF Conference on Computer Vision and Pattern Recognition*, pp. 21694–21704, 2023. [2](#)
- [58] W. Zhang, Y. Liu, X. Zheng, and L. Wang, “Goodsam: Bridging domain and capacity gaps via segment anything model for distortion-aware panoramic semantic segmentation,” in *IEEE/CVF Conference on Computer Vision and Pattern Recognition, CVPR 2024, Seattle, WA, USA, June 16-22, 2024*, pp. 28264–28273, IEEE, 2024. [2](#)
- [59] W. Zhang, Y. Liu, X. Zheng, and L. Wang, “Goodsam++: Bridging domain and capacity gaps via segment anything model for panoramic semantic segmentation,” *CoRR*, vol. abs/2408.09115, 2024.
- [60] X. Zheng, Y. Lyu, L. Jiang, J. Zhou, L. Wang, and X. Hu, “MAGIC++: efficient and resilient modality-agnostic semantic segmentation via hierarchical modality selection,” *CoRR*, vol. abs/2412.16876, 2024.
- [61] C. Liao, X. Zheng, Y. Lyu, H. Xue, Y. Cao, J. Wang, K. Yang, and X. Hu, “Memorysam: Memorize modalities and semantics with segment anything model 2 for multi-modal semantic segmentation,” *CoRR*, vol. abs/2503.06700, 2025.
- [62] C. Liao, K. Lei, X. Zheng, J. Moon, Z. Wang, Y. Wang, D. P. Paudel, L. V. Gool, and X. Hu, “Benchmarking multi-modal semantic segmentation under sensor failures: Missing and noisy modality robustness,” *CoRR*, vol. abs/2503.18445, 2025.
- [63] D. Zhong, X. Zheng, C. Liao, Y. Lyu, J. Chen, S. Wu, L. Zhang, and X. Hu, “Omnisam: Omnidirectional segment anything model for UDA in panoramic semantic segmentation,” *CoRR*, vol. abs/2503.07098, 2025.
- [64] X. Zheng and L. Wang, “Eventdance++: Language-guided unsupervised source-free cross-modal adaptation for event-based object recognition,” *CoRR*, vol. abs/2409.12778, 2024. [2](#)
- [65] Y. Liang, R. Wakaki, S. Nobuhara, and K. Nishino, “Multi-modal material segmentation,” in *Proceedings of IEEE/CVF CVPR*, pp. 19800–19808, 2022. [2](#), [6](#), [7](#)
- [66] T. Broedermann, C. Sakaridis, D. Dai, and L. Van Gool, “Hrfuser: A multi-resolution sensor fusion architecture for 2d object detection,” in *IEEE International Conference on Intelligent Transportation Systems*, pp. 4159–4166, 2023. [2](#)
- [67] S. Wei, C. Luo, and Y. Luo, “Mmanet: Margin-aware distillation and modality-aware regularization for incomplete multimodal learning,” in *Proceedings of the IEEE/CVF Conference on Computer Vision and Pattern Recognition*, pp. 20039–20049, 2023.
- [68] Y. Man, L.-Y. Gui, and Y.-X. Wang, “Bev-guided multi-modality fusion for driving perception,” in *Proceedings of the IEEE/CVF Conference on Computer Vision and Pattern Recognition*, pp. 21960–21969, 2023. [2](#)
- [69] J. Zhang, H. Liu, K. Yang, X. Hu, R. Liu, and R. Stiefelhagen, “Cmx: Cross-modal fusion for rgb-x semantic segmentation with transformers,” *arXiv:2203.04838*, 2022. [2](#)
- [70] R. Liu, J. Zhang, K. Peng, Y. Chen, K. Cao, J. Zheng, M. S. Sarfraz, K. Yang, and R. Stiefelhagen, “Fourier prompt tuning for modality-incomplete scene segmentation,” in *IEEE Intelligent Vehicles Symposium*, pp. 961–968, 2024. [2](#), [5](#)
- [71] Y.-L. Lee, Y.-H. Tsai, W.-C. Chiu, and C.-Y. Lee, “Multi-modal prompting with missing modalities for visual recognition,” in *Proceedings of the IEEE/CVF Conference on Computer Vision and Pattern Recognition*, pp. 14943–14952, 2023. [5](#)
- [72] R. Bachmann, D. Mizrahi, A. Atanov, and A. Zamir, “Multimae: Multi-modal multi-task masked autoencoders,” in *European Conference on Computer Vision*, pp. 348–367, Springer, 2022. [5](#)
- [73] T. Brödermann, D. Bruggemann, C. Sakaridis, K. Ta, O. Liagouris, J. Corkill, and L. Van Gool, “Muses: The multi-sensor semantic perception dataset for driving under uncertainty,” in *ECCV*, pp. 21–38, Springer, 2025. [6](#)
- [74] J. Zhang, H. Liu, K. Yang, X. Hu, R. Liu, and R. Stiefelhagen, “Cmx: Cross-modal fusion for rgb-x semantic segmentation with transformers,” *IEEE Transactions on intelligent transportation systems*, 2023. [6](#)
- [75] T. Brödermann, D. Bruggemann, C. Sakaridis, K. Ta, O. Liagouris, J. Corkill, and L. Van Gool, “Muses: The multi-sensor semantic perception dataset for driving under uncertainty,” in *Proceedings of the European Conference on Computer Vision*, 2024. [6](#), [8](#)